

QUASI-LONG-RANGE ORDER IN RANDOM-ANISOTROPY HEISENBERG MODELS

Ronald Fisch

Department of Physics

Washington University

St. Louis, Missouri 63130

(Submitted to Physical Review B, 5 January 1998)

Monte Carlo simulations have been used to study a discretized Heisenberg ferromagnet (FM) with random uniaxial single-site anisotropy on $L \times L \times L$ simple cubic lattices, for L up to 64. The spin variable on each site is chosen from the twelve [110] directions. The random anisotropy has infinite strength and a random direction on a fraction x of the sites of the lattice, and is zero on the remaining sites. In many respects the behavior of this model is qualitatively similar to that of the corresponding random-field model. Due to the discretization, for small x at low temperature there is a [110] FM phase. For $x > 0$ there is an intermediate quasi-long-range ordered (QLRO) phase between the paramagnet and the ferromagnet, which is characterized by a $|\mathbf{k}|^{-3}$ divergence of the magnetic structure factor $S(\mathbf{k})$ for small \mathbf{k} , but no true FM order. At the transition between the paramagnetic and QLRO phases $S(\mathbf{k})$ diverges like $|\mathbf{k}|^{-2}$. The limit of stability of the QLRO phase is somewhat greater than $x = 0.5$. For x close to 1 the low temperature form of $S(\mathbf{k})$ can be fit by a Lorentzian, with a correlation length estimated to be 11 ± 1 at $x = 1.0$ and 25 ± 5 at $x = 0.75$.

PACS numbers: 75.10.Nr, 64.60.Cn, 75.40.Mg, 75.50.Lk

I. INTRODUCTION

The Heisenberg model with random uniaxial single-site anisotropy is considered to be the proper model for studying amorphous alloys^{1,2} of non- S -state rare earths (RE) and transition metals (TM), such as $\text{Tb}_x\text{Fe}_{1-x}$. The model was introduced by Harris, Plischke and Zuckermann,³ who performed a mean-field calculation and found a ferromagnetic (FM) phase at low temperature. It was shown later by Pelcovits, Pytte and Rudnick,⁴ using an argument parallel to that of Imry and Ma⁵ for the random field case, that such a FM phase is not stable in three dimensions.

The actual behavior of this model in three dimensions has remained a subject of controversy. It was argued by some workers^{4,6-8} that there should be a low temperature Ising spin-glass phase, but the numerical evidence for this was never convincing.^{9,10} It has recently been shown by Migliorini and Berker¹¹ that in three dimensions the Ising spin glass is destabilized by a random field. The spin glass phase, as it is usually envisioned, has spontaneously broken time-reversal symmetry (i.e. the time-average expectation values of local moments do not vanish). Therefore, one would expect that it should also be destabilized by random uniaxial anisotropy.

An alternative scenario, first proposed by Aharony and Pytte,¹² is that at low temperature there is a phase characterized by an infinite magnetic susceptibility and a power-law decay of two-spin correlations as a function of the distance between the two spins, but no true FM long-range order. This power-law decay of the two-spin correlations is called quasi-long-range order (QLRO). In the approximation of Aharony and Pytte, and its later elaboration by Goldschmidt and Aharony,¹³ it is claimed that the infinite-susceptibility phase occurs in the presence of random anisotropy, but not in the presence of a random field. This is rather problematic, as it requires that the infinite-susceptibility phase not break time-reversal symmetry. The relationship between the ordered states of random-field and random-anisotropy models is well known, as it provides the key step in the argument of Pelcovits, Pytte and Rudnick.⁴

In the last few years, Monte Carlo calculations have revealed that for the $n = 2$ case (where n is the number of spin components) there is a low temperature phase with power-law decay of two-spin correlations (which will be referred to as the QLRO phase) for both the random uniaxial anisotropy¹⁴ and random field¹⁵ in three dimensions. The QLRO phase is characterized by the small-wavenumber behavior of the magnetic structure factor

$$S(\mathbf{k}) = \langle [|\mathbf{M}(\mathbf{k})|^2] \rangle \quad , \quad (1)$$

where the expectation value $\langle \rangle$ indicates a thermal average and $[]$ is an average over the alloy disorder. $\mathbf{M}(\mathbf{k})$ is the Fourier transform of the magnetization. With the random field it was found that in the QLRO phase the small \mathbf{k} behavior of $S(\mathbf{k})$ goes as \mathbf{k}^{-3} , and with the random uniaxial anisotropy it goes as $\mathbf{k}^{-2.4}$. A spin-wave theory analysis would predict that this behavior should be the same. Thus the fact that the power law is found to be different in the

two cases demonstrates that vortex lines are controlling the behavior for $n = 2$ with random anisotropy. The $n = 2$ case with three-fold (or higher) random anisotropy retains a stable FM phase in three dimensions.¹⁶

Other papers which indicate the presence of QLRO for $n = 2$ are the Monte Carlo calculation of Gingras and Huse¹⁷ for the random field case, the high temperature susceptibility series of Fisch and Harris¹⁸ for the random anisotropy case, and the replica-symmetry breaking analysis of Giamarchi and Le Doussal.¹⁹ The latter work actually studies the closely related problem of randomly pinned vortex lines in a dirty type-II superconductor.²⁰

The existence of QLRO for $n = 2$ is not a big surprise, given our previous experience with the Kosterlitz-Thouless phase in the (nonrandom) two-dimensional XY model. However, the Aharony-Pytte-Goldschmidt^{12,13} calculations find an infinite-susceptibility phase for any finite value of n , independent of the existence of any topological defects. Recently, a Monte Carlo calculation by the current author²¹ found a QLRO phase with an $S(\mathbf{k})$ which goes as \mathbf{k}^{-3} for the $n = 3$ model in a random field in three dimensions. Here we will extend this work to the case of $n = 3$ spins with random anisotropy, and we will find the same result for the small \mathbf{k} behavior of $S(\mathbf{k})$ as for the random field.

II. DISCRETIZED HEISENBERG MODEL WITH RANDOM ANISOTROPY

The Hamiltonian we study in this work is the obvious modification of the one previously used for the $n = 3$ random field model.²¹ It consists of a FM Heisenberg exchange term, with the addition of a cubic single-ion anisotropy term and a random-anisotropy term due to the alloy disorder. Thus the form of the Hamiltonian is

$$H = -J \sum_{\langle ij \rangle} \sum_{\alpha=1}^3 S_i^\alpha S_j^\alpha - K \sum_i \sum_{\alpha=1}^3 (S_i^\alpha)^4 - D \sum_{i'} ((\mathbf{S}_{i'} \cdot \mathbf{n}_{i'})^2 - 1), \quad (2)$$

where the sites i form a simple cubic lattice and $\langle ij \rangle$ indicates a sum over nearest neighbors. The α are spin indices, each $\mathbf{n}_{i'}$ is an independently chosen random unit vector, and the i' sites are a randomly chosen subset of the lattice containing a fraction x of the sites.

The i' sites represent the sites of the RE atoms, while the remaining sites of the lattice contain the TM atoms. This ignores the fact that the RE-TM alloys of interest here are amorphous rather than crystalline, but it is a reasonable first approximation. Since the atoms are assumed to be immobile, the $\mathbf{n}_{i'}$ do not change with time. In this work we will study the limit in which D is taken to infinity. The random anisotropy term is then a projection operator, and the spin on each of the i' sites is restricted to two states, parallel and antiparallel to the vector $\mathbf{n}_{i'}$. For simplicity, we will assume that all of the spins are unit vectors and that the exchange couplings J between all pairs of nearest neighbor spins are identical. Our assumed values for the couplings are not close to the actual values in RE-TM alloys,² but they should still give the qualitative behavior correctly, due to universality.

There are several reasons for including the cubic single-ion anisotropy term in the Hamiltonian. The first is a matter of convenience. In order to improve the efficiency of the Monte Carlo program,^{21,22} and to make it easy to store states of the system for later analysis, we are going to discretize the phase space of the model. For each spin variable \mathbf{S}_i and each random anisotropy axis $\mathbf{n}_{i'}$, we restrict the allowed states to be the twelve [110] unit vectors. We will refer to this discretization as the \mathbf{O}_{12} model. This discretization induces an effective cubic single-ion anisotropy term in the Hamiltonian. The second reason is that the experimental samples of amorphous RE-TM alloys are sputtered films which have some growth-induced anisotropy.²³ Understanding the effects of this weak anisotropy is a worthwhile exercise. The existence of the growth-induced anisotropy is crucial for the use of these films as magneto-optical memory devices.²⁴ The third reason is that besides the amorphous RE-TM alloys, we are also interested in crystalline spin-glass alloys like CuMn,^{14,25} where a cubic single-ion anisotropy is present in the real materials.

Another discretized three-dimensional $n = 3$ Hamiltonian which combines cubic single-ion anisotropy and random uniaxial anisotropy has been studied previously.²⁶ In that case only six states (the [100] unit vectors) were used. Although the six-state discretization is too coarse to serve as a quantitative approximation to the Heisenberg model, some indications of a QLRO phase were found in that work.

A discussion from a renormalization-group viewpoint of the effects of having both a crystalline anisotropy and random uniaxial anisotropy has been given by Mukamel and Grinstein.²⁷ They argued that a QLRO phase could exist in this case between the FM and the paramagnet (PM), as was later found by the Monte Carlo calculation for the $n = 2$ case. They also discussed the difference between a discretized model in which all of the allowed axes are mutually orthogonal, such as the six-state model for $n = 3$, and finer discretizations such as the \mathbf{O}_{12} model, which are expected to provide approximations to a model without the crystalline anisotropy.

Since our \mathbf{O}_{12} discretization of the spin variables automatically builds a cubic anisotropy into the free energy, and we are primarily trying to understand the qualitative aspects of the ordering and not attempting a quantitative model

of a particular experiment, we do not keep the K term in the Hamiltonian explicitly. Thus, the Hamiltonian is reduced to the simple form

$$H = -J \sum_{\langle ij \rangle} \mathbf{S}_i \cdot \mathbf{S}_j \quad . \quad (3)$$

The random anisotropy term has been reduced to the constraint⁹ that for each site in the i' set the spin $\mathbf{S}_{i'}$ has only two allowed states, either parallel or antiparallel to the vector $\mathbf{n}_{i'}$.

III. MONTE CARLO CALCULATION

Because all of the \mathbf{S}_i are chosen from the [110] states, Eq. (3) has the useful property that the energy of every state is an integral multiple of $1/2$. Thus it becomes easy to write a Monte Carlo program to study Eq. (3) which uses integer arithmetic to calculate energies. This, plus the fact that each spin has only twelve possible states, gives substantial improvements in performance over working with the general form of Eq. (2), for both memory size and speed. It is also possible to use integer arithmetic if D is chosen to be an integer.²⁶

The Monte Carlo program used two linear congruential pseudorandom number generators. In order to avoid unwanted correlations, the decision of whether or not a state was in the i' set was done using one of the generators, and the choice of the vector $\mathbf{n}_{i'}$ was made using the other. A heat bath method was used for flipping the spins, which at each step reassigned the value of a spin to one of its two allowed states if it was a member of the i' set, or to one of the twelve [110] states if it was not, weighted according to the Boltzmann factors and independent of the prior state of the spin.

$L \times L \times L$ simple cubic lattices with periodic boundary conditions were used throughout. The values of L used ranged from 16 to 64. Away from any T_c the samples were typically run for 10,240 Monte Carlo steps per spin (MCS) at each T , with sampling after each 10 MCS. Near a T_c they were run several times longer. The initial part of each data set was discarded for equilibration. In some cases, two different random field configurations with a given L were studied for a given $x > 0$. This gives a rather crude estimate of the L dependence of the various thermodynamic properties. We are forced to go to large L for this problem by crossover effects. To do a high precision finite-size-scaling analysis would require studying many samples at each L , which is very time-consuming for large L .

Due to our discretization of the spins, in a ground state with $x \leq 0.25$ essentially all of the spins are as aligned as possible along one of the [110] directions, consistent with the restriction that each i' spin be in one of its two allowed states. Thus, in these cases it is easy to equilibrate the system at low temperatures by starting from an ordered configuration. For $x = 0.25$ a sample with small L will spontaneously nucleate a [110] FM state upon cooling, but for $L = 64$ this does not happen in the time available. When an $L = 64$ sample with $x = 0.25$ is slowly cooled to $T/J = 0.5625$ it nucleates a polydomain state. For $x \geq 0.5$, where the ground state is not a [110] FM state, it becomes extremely difficult to equilibrate large lattices at low temperatures.

In the absence of any external field, the rotation of \mathbf{M} between different [110] directions is a slow process. In the presence of the random anisotropy the different [110] ferromagnetic Gibbs states have different energies. Because all of these twelve minima are equivalent, on the average, there is no need for the Monte Carlo program to average over them. If the system is started in a high-energy [110] direction, it will eventually jump to a more favorable direction, unless T is so low that this does not happen in the time available.

IV. NUMERICAL RESULTS

For $x = 0$ there is no random anisotropy, and results for this case were presented earlier.²¹ Monte Carlo simulations with the random anisotropy were obtained for $x = 0.125, 0.25, 0.5, 0.75$ and 1.0 . A approximate picture of the phase diagram obtained from these results is shown in Fig. 1. The limit of stability of the [110] FM ground state is between $x = 0.25$ and $x = 0.5$. The QLRO phase exists for $x \leq 0.5$, but is unstable at $x = 0.75$.

The [111] FM phase, which is stable at $x = 0$,²¹ should also extend to small positive values of x . The domain walls in this phase are broad and have a low cost in free energy. It is difficult to obtain meaningful numerical results for very small x , due to crossover effects.²⁸ The [111] FM-QLRO phase boundary was not observed directly, and its existence is shown in Fig. 1 as a dotted line. Although for small x the effective cubic anisotropy induced by our discretization favors the [111] directions, for x near 0.5 the effective anisotropy favors the [100] directions. Consequently, near $x = 0.25$ the effective cubic anisotropy is very small. There is probably a [100] FM low temperature phase near $x = 0.5$. However, because it is so difficult to equilibrate large L samples in this region of the phase diagram, the details are very uncertain.

The QLRO-to-PM transition is second order for $x \leq 0.5$. The energy at T_c remains nearly constant along this part of the transition line, decreasing very slowly as x increases. The shift of T_c with x is surprisingly small here; at $x = 0$

$$\frac{d}{dx} \left(\frac{T_c(x)}{T_c(0)} \right) = -0.12 \pm 0.02 \quad . \quad (4)$$

Similar effects were observed in the $n = 2$ random anisotropy case,¹⁴ but the random field cases are significantly different.²¹ At some $x > 0.5$ T_c begins to drop rapidly, and by $x = 0.75$ the QLRO phase has disappeared. The details of the sharp drop in T_c are not clear, and they may depend on the presence of the effective cubic anisotropy, without which the [100] FM phase would be stable.

Because in the presence of the random anisotropy the expectation values of the energies of different bonds are not the same, one certainly does not expect the energy at T_c to remain exactly constant, independent of x . Unlike the random field, however, which causes spins to have nonvanishing expectation values even at high temperatures, the random uniaxial anisotropy does not produce major qualitative changes in the PM phase. Therefore, it is not unreasonable that the limit of stability of the PM phase occurs at about the same value of the nearest neighbor two-spin correlation function, which is the energy in this model. Recall that in a tree-diagram summation the energy at T_c of the classical n -vector ferromagnet depends only on the lattice structure, and is independent of the number of spin components.

For the $n = 2$ random anisotropy model it was found¹⁴ that the QLRO phase exists on a simple cubic lattice²⁹ even for $x = 1$, but here we see that QLRO is less stable for $n = 3$ random anisotropy. Although the $n = 4$ case is not (to the author's knowledge) of any experimental relevance, it would be quite interesting to know if it is possible to have a QLRO phase for small nonzero x in that case, and for larger finite values of n . The author sees no reason why this should not be so. Some authors³⁰ have argued for the importance of hedgehog excitations in three-dimensional $n = 3$ models, but this does not seem to hold up under detailed scrutiny.³¹ In a lattice model one can obtain equivalent effects by replacing the hedgehog fugacity with a nontopological multispin interaction, and this multispin interaction can be extended in a straightforward way to the $n = 4$ case.³²

The behavior of the specific heat as x is increased is shown in Fig. 2. The data displayed were obtained by numerically differentiating the calculated values of the energy with respect to T . The specific heat was also computed by calculating the fluctuations in the energy at fixed temperature, yielding similar but noisier results. We see that the data for different samples with the same value of x agree fairly well, although some differences are visible near the phase transitions.

The sharp peaks which occur²¹ for $x = 0$ become rounded as x increases, and they move to lower T . At $x = 0.125$ the behavior of the specific heat at the QLRO-to-PM transition can be approximated by an effective critical specific heat exponent $\alpha_{eff} = -0.45$, with an amplitude ratio of 2.5. The transition out of the [110] FM phase still appears to be first order at $x = 0.125$, although the latent heat is too small to measure accurately.³³ It is likely that this transition actually goes into the [111] FM phase. At $x = 0.25$ there is substantial hysteresis at the [110] FM-to-QLRO transition, which makes an accurate determination of the equilibrium thermodynamic properties near this transition impossible. The specific heat near the QLRO-to-PM transition at $x = 0.25$, shown in Fig. 2(b), is remarkably similar to the specific heat recently reported for real amorphous RE-TM films.² The effective value of the critical specific heat exponent is now $\alpha_{eff} = -0.6$, and the amplitude ratio is again about 2.5. It is well known³⁴ that the introduction of randomness gives rise to effective critical exponents that appear to vary with x . By $x = 0.5$ the specific heat peak has become rather smeared out, but it still seems to be centered at the QLRO-to-PM transition. The shoulder on the low temperature side of the peak in Fig. 2(c) may be due to a transition from the QLRO phase into a [100] FM phase.

Looking at the dependence of $\langle |\mathbf{M}| \rangle$ on x and L provides additional insight. The data for $x = 0.25$ and $x = 0.5$ are shown in Fig. 3. In the [110] FM phase, $\langle |\mathbf{M}| \rangle$ is almost independent of L , except very close to T_c . In the [111] and [100] FM phases, $\langle |\mathbf{M}| \rangle$ becomes independent of L only when L is larger than the domain-wall thickness. In practice we do not satisfy this condition, and for accessible L it becomes very difficult to distinguish the [111] and [100] FM phases from the QLRO phase. In the QLRO phase, $\langle |\mathbf{M}| \rangle$ decreases slowly as L increases, probably decaying as $1/\log(L)$. In the PM phase, $\langle |\mathbf{M}| \rangle$ decreases as $(L/\xi)^{-3/2}$, where ξ is the ferromagnetic correlation length.

In Fig. 3 we see that for both values of x the variation of $\langle |\mathbf{M}| \rangle$ with T becomes increasingly sharp as L increases. If one looks at finite-size scaling plots (not shown), there is substantial scatter due to sample-to-sample fluctuations. However, in both cases the finite-size scaling is consistent with a divergence of ξ as T approaches T_c in the PM phase, with an effective value of β/ν (and therefore of η) which is indistinguishable from the standard $n = 3$ Heisenberg critical point value.³⁵ The data can also be fit with $\eta = 0$. The effective values of ν are, however, about 0.8 at $x = 0.25$ and 1.0 at $x = 0.5$. Note that if one uses the effective value of ν found here for $x = 0.25$ and the effective value of α found in the specific heat, the Josephson relation $d\nu = 2 - \alpha$ is satisfied within the accuracy of the estimates. There is no reason, however, why effective exponents should satisfy scaling relations exactly.

We can get valuable information by looking at the magnetic structure factor $S(\mathbf{k})$. The structure factor can be

measured by X-ray and neutron scattering experiments. Near T_c the small-wavenumber behavior of the structure factor is expected to have the form

$$S(\mathbf{k}) \approx A/(1/\xi^2 + |\mathbf{k}|^2)^{1-\eta/2} \quad . \quad (5)$$

As T approaches T_c in the PM phase, ξ is expected to diverge like $(T - T_c)^{-\nu}$. $S(\mathbf{k})$ at T_c for an $L = 64$ sample with $x = 0.25$ is shown on a log-log plot in Fig. 4. The exponent η is seen to be very close to zero; this is the same result that was found for this exponent in the $n = 2$ random anisotropy case.¹⁴

Inside the QLRO phase $S(\mathbf{k})$ appears to take on the form

$$S(\mathbf{k}) \approx A/(1/\xi^2 + |\mathbf{k}|^2) + B/(1/\xi^2 + |\mathbf{k}|^2)^{1-\eta_0/2} \quad , \quad (6)$$

with $\eta_0 = -1$, independent of T . The B term has replaced the δ -function which would be found in the structure factor of a ferromagnet. The coefficient B goes to zero continuously as T approaches T_c from below, presumably with an exponent 2β . At $x = 0.25$ where the effective cubic anisotropy is small, ξ is found to be immeasurably large in the QLRO phase, which means that it must be large compared to $L = 64$.

This is shown in Fig. 5, which displays $S(\mathbf{k})$ data from the same $L = 64$ sample as in Fig. 4, but for lower T . The data set shown with the + symbols was obtained by slowly cooling the lattice from above T_c to $T/J = 0.6875$. After discarding the initial part of the run, this state appears stationary on a timescale of 50,000 MCS. It has $\langle |\mathbf{M}| \rangle = 0.419$, and an energy of -1.9992 . The fit of this data to a straight line with a slope of -3 is excellent. The remaining data shown here were generated using a cold start initial condition, with the direction of \mathbf{M} chosen to be approximately the same as for the slowly cooled state. At $T/J = 0.5$, which is within the [110] FM phase, $\langle |\mathbf{M}| \rangle = 0.812$ and $S(\mathbf{k})$ is rather flat at nonzero \mathbf{k} . Upon warming this state up to $T/J = 0.5625$, which is approximately equal to the FM-QLRO transition point, $\langle |\mathbf{M}| \rangle$ has decreased to 0.757, and $S(\mathbf{k})$ has increased at nonzero \mathbf{k} .

Using a cold start initial condition at $T/J = 0.6875$ results in a state which does not relax to equilibrium on accessible timescales. The data shown in Fig. 5 with the diamond symbols fall on top of the equilibrium (slow-cooled) data for $\mathbf{k} \geq 0.1$, but they are flat at smaller \mathbf{k} , where relaxation times are long. These data have $\langle |\mathbf{M}| \rangle = 0.599$ and an energy of -2.0045 , but there is a clear trend of decreasing $\langle |\mathbf{M}| \rangle$ and increasing energy with time. The rounded peak²⁵ and slow relaxation³⁶ of this state are quite reminiscent of the field-cooled state in the spin-glass phase of CuMn alloys.

For $x \geq 0.75$ the ferromagnetic correlation length does not become larger than accessible values of L at any temperature, and $S(\mathbf{k})$ can be fit by a simple Lorentzian form (*i.e.* setting $\eta = 0$ in Eq. (5)). This is shown in Fig. 6. For $x = 0.75$ we display data taken at $T/J = 1.15625$ for an $L = 64$ sample, using both slow cooling and cold start initial conditions. This value of T is slightly below what our extrapolation from small x would lead us to expect T_c would be. Although there is a substantial peak in $S(\mathbf{k})$, the value of ξ (measured in lattice units) appears to be 25 ± 5 , and it does not increase as T is lowered.

Data for two $L = 32$ samples with $x = 1$ at $T/J = 0.75$ using slow cooling are shown in Fig. 6(b). Here the value of ξ is 11 ± 1 , in excellent agreement with earlier estimates for the $x = 1$ model with $n = 3$ isotropic random anisotropy.^{9,10} For $x = 1$, ξ becomes essentially temperature-independent below about $T/J = 0.9$, but there is no evidence of singular behavior at any T . Given the recent results of Migliorini and Berker,¹¹ the author does not believe that there is any phase transition at $T > 0$ in this model when $x \geq 0.75$. Although no attempt was made to find the exact ground states of these samples, the estimated ground state energy for the \mathbf{O}_{12} model at $x = 1$ is $-1.12 \pm 0.01J$, essentially equal to its value in the isotropic random anisotropy case.

V. DISCUSSION

The integral of $S(\mathbf{k})$ over \mathbf{k} is proportional to the total neutron-scattering cross-section, which is finite. Because $|\mathbf{k}|^{-3}$ is not an integrable singularity in three dimensions, either ξ must become finite, albeit extremely large, below T_c where B is nonzero, or else η_0 must be modified slightly to make the integral converge. In the presence of some crystalline or growth-induced nonrandom anisotropy, it is natural to expect that ξ becomes finite, just as it does in a nonrandom ferromagnet below T_c .³² Although it has become traditional to fit neutron-scattering data for $S(\mathbf{k})$ in random-field and random-anisotropy magnets to a Lorentzian plus Lorentzian² form, this is based on a theoretical preconception. It has been known for a long time that Eq. (6) will serve to fit the data in some cases,³⁷ while in others^{1,37} the 3 in the exponent should be replaced by 2.4. A value of 2.4 in this exponent is precisely the value found for the $n = 2$ random-anisotropy model,¹⁴ and thus should be expected in the presence of easy-plane anisotropy. The $|\mathbf{k}|^{-3}$ behavior of $S(\mathbf{k})$ for $n = 3$ is the same exponent for both the random-anisotropy and random-field cases. Therefore, we have no reason to believe that the presence of hedgehog singularities is essential for the QLRO when

$n = 3$. There seems to be no reason why QLRO should not exist for larger finite values of n , as originally predicted by Aharony and Pytte.¹²

The magnetic susceptibility is

$$\chi^{\alpha\beta} = (NT)^{-1} \sum_{i,j=1}^N [\langle S_i^\alpha S_j^\beta \rangle] - [\langle S_i^\alpha \rangle \langle S_j^\beta \rangle] \quad . \quad (7)$$

The Aharony-Pytte-Goldschmidt^{12,13} analysis predicts that at small wavenumbers its Fourier transform, $\chi(\mathbf{k})$ will behave like $|\mathbf{k}|^{-2}$. If time-reversal symmetry is unbroken, then the $[\langle S_i^\alpha \rangle \langle S_j^\beta \rangle]$ terms all vanish, and the trace of $\chi(\mathbf{k})$ is proportional to $S(\mathbf{k})$. Thus Aharony-Pytte-Goldschmidt implicitly predicts that $S(\mathbf{k})$ goes like $|\mathbf{k}|^{-2}$ in the QLRO phase, which is not correct. Its prediction for $\chi(\mathbf{k})$ in the QLRO phase is, however, probably correct in the absence of any crystalline anisotropy. To check this numerically would require very long runs, in order to compute the $[\langle S_i^\alpha \rangle \langle S_j^\beta \rangle]$ terms accurately. This has not been attempted here.

It is likely that the reason why Aharony-Pytte-Goldschmidt fails to predict the QLRO for the random-field case is also its incorrect handling of the $[\langle S_i^\alpha \rangle \langle S_j^\beta \rangle]$ terms. For the random-field case these terms are nonzero even in the PM phase.

The FM phases shown in Fig. 1 exist because of the anisotropy induced by our discretization. It would be very helpful to repeat this calculation using an alternative discretization, such as Rapaport's 30-state model,²² which has icosahedral symmetry. It would also be desirable to study a continuous-spin binary alloy model with a fully isotropic distribution of the random anisotropy. This would be very difficult to manage for large lattices, unless a way can be found to adapt the cluster Monte Carlo algorithm³⁸ to include the random anisotropy. When $x > 0$ the Hamiltonian no longer has any planes of reflection symmetry, even though it is still inversion-symmetric.

VI. CONCLUSION

In this work we have used Monte Carlo simulations to study the \mathbf{O}_{12} version of the diluted random-anisotropy ferromagnet in three dimensions. We have found that there are two types of ordered phases, just as in the $n = 2$ case. In addition to the anisotropy-stabilized ferromagnet, we find an intermediate QLRO phase displaying a $|\mathbf{k}|^{-3}$ behavior of the magnetic structure factor. This is the same behavior which has been found for $n = 3$ random-field model. The critical exponent η , which characterizes the two-spin correlations on the QLRO-to-PM critical line, has a value which is indistinguishable from zero. The results should be applicable to a variety of experimental systems, including amorphous RE-TM alloys and CuMn-type spin-glass alloys.

ACKNOWLEDGMENTS

This work was undertaken after the author was shown a preliminary version of the results of Hellman, Abarra and Shapiro. The author is grateful to Frances Hellman for extensive discussions of these results. He also thanks Phil Anderson, Nihat Berker, Yadin Goldschmidt, Brooks Harris, David Huse and Tom Lubensky for helpful discussions.

¹ S. J. Pickart, J. J. Rhyne and H. A. Alperin, Phys. Rev. Lett. **33**, 424 (1974); S. J. Pickart, H. A. Alperin and J. J. Rhyne, Phys. Lett. **64A**, 377 (1977).

² F. Hellman, E. N. Abarra and A. L. Shapiro, submitted to Phys. Rev. B.

³ R. Harris, M. Plischke and M. J. Zuckermann, Phys. Rev. Lett. **31**, 160 (1973).

⁴ R. A. Pelcovits, E. Pytte and J. Rudnick, Phys. Rev. Lett. **40**, 476 (1978).

⁵ Y. Imry and S.-K. Ma, Phys. Rev. Lett. **35**, 1399 (1975).

⁶ J.-H. Chen and T. C. Lubensky, Phys. Rev. **B 16**, 2106 (1977).

⁷ E. M. Chudnovsky, W. M. Saslow and R. A. Serota, Phys. Rev. **B 33**, 251 (1986).

⁸ A. Chakrabarti, J. Appl. Phys. **63**, 3735 (1988).

⁹ C. Jayaprakash and S. Kirkpatrick, Phys. Rev. **B 21**, 4072 (1980).

¹⁰ R. Fisch, Phys. Rev. **B 42**, 540 (1990).

- ¹¹ G. Migliorini and A. N. Berker, Phys. Rev. **B 57**, 426 (1998).
- ¹² A. Aharony and E. Pytte, Phys. Rev. Lett. **45**, 1583 (1980).
- ¹³ Y. Y. Goldschmidt and A. Aharony, Phys. Rev. **B 32**, 264 (1985).
- ¹⁴ R. Fisch, Phys. Rev. **B 51**, 11 507 (1995).
- ¹⁵ R. Fisch, Phys. Rev. **B 55**, 8211 (1997).
- ¹⁶ R. Fisch, Phys. Rev. **B 46**, 242 (1992).
- ¹⁷ M. J. P. Gingras and D. A. Huse, Phys. Rev. **B 53**, 15 193 (1996).
- ¹⁸ R. Fisch and A. B. Harris, Phys. Rev. **B 41**, 11 305 (1990).
- ¹⁹ T. Giamarchi and P. Le Doussal, Phys. Rev. Lett. **72**, 1530 (1994); Phys. Rev. **52**, 1242 (1995).
- ²⁰ A. I. Larkin, Zh. Eksp. Teor. Fiz. **58**, 1466 (1970) [Sov. Phys. - JETP **31**, 784 (1970)].
- ²¹ R. Fisch, Phys. Rev. **B 57**, 269 (1998).
- ²² D. C. Rapaport, J. Phys. **A 18**, L667 (1985).
- ²³ S. N. Cheng and M. H. Kryder, J. Appl. Phys. **69**, 7202 (1991).
- ²⁴ P. Hansen and H. Heitmann, IEEE Trans. Magn. **MAG-25**, 4390 (1989).
- ²⁵ S. A. Werner, Comments Cond. Matt. Phys. **15**, 55 (1990).
- ²⁶ R. Fisch, Phys. Rev. **B 48**, 15 764 (1993).
- ²⁷ D. Mukamel and G. Grinstein, Phys. Rev. **B 25**, 381 (1982).
- ²⁸ K. Binder and H.-P. Deutsch, Europhys. Lett. **18**, 667 (1992).
- ²⁹ The existence of QLRO at $x = 1$ is lattice dependent. For example, if a ferromagnetic second neighbor exchange coupling was added, then one might expect a QLRO phase for $n = 3$ at $x = 1$.
- ³⁰ M.-h. Lau and C. Dasgupta, J. Phys. **A 21**, L51 (1988); Phys. Rev. **B 39**, 7212 (1989).
- ³¹ C. Holm and W. Janke, J. Phys. **A 27** 2553 (1994).
- ³² R. Fisch, J. Appl. Phys. **79**, 5088 (1996).
- ³³ For the lattices sizes studied here, the sample-to-sample fluctuations are comparable to the estimated latent heat itself.
- ³⁴ G. S. Rushbrooke, R. A. Muse, R. L. Stephenson and K. Pirnie, J. Phys **C 5**, 3371 (1972).
- ³⁵ J. C. Le Guillou and J. Zinn-Justin, Phys. Rev. **B 21**, 3976 (1980); J. Phys. Lett. (Paris) **46**, L137 (1985).
- ³⁶ P. Nordblad, P. Svedlindh, L. Lundgren and L. Sandlund, Phys. Rev. **B 33**, 645 (1986).
- ³⁷ H. Yoshizawa *et al.*, Phys. Rev. Lett. **48**, 438 (1982).
- ³⁸ U. Wolff, Phys. Rev. Lett. **62**, 361 (1989).

FIG. 1. Phase diagram of the dilute random-anisotropy \mathbf{O}_{12} model on simple cubic lattices, showing the paramagnetic (PM), ferromagnetic (FM), and quasi-long-range order (QLRO) phases. The plotting symbols show estimates obtained from the Monte Carlo data. The solid lines indicate first-order transitions, and the dashed lines indicate second-order transitions. The dotted lines represent transitions which are inferred indirectly, and whose locations are rather uncertain.

FIG. 2. Specific heat vs. temperature for the dilute random-anisotropy \mathbf{O}_{12} model on $L \times L \times L$ simple cubic lattices. (a) $x = 0.125$; (b) $x = 0.25$; (c) $x = 0.5$.

FIG. 3. Magnetization vs. temperature for the dilute random-anisotropy \mathbf{O}_{12} model on $L \times L \times L$ simple cubic lattices. The y -axis is scaled logarithmically. (a) $x = 0.25$; (b) $x = 0.5$.

FIG. 4. Angle-averaged magnetic structure factor at the PM-to-QLRO transition for the dilute random-anisotropy \mathbf{O}_{12} model on a $64 \times 64 \times 64$ simple cubic lattice with $x = 0.25$, log-log plot. The points show averaged data from 4 states sampled at 10,240 MCS intervals. The line has a slope of -2.00 .

FIG. 5. Angle-averaged magnetic structure factor near the [110] FM-to-QLRO transition for the dilute random-anisotropy \mathbf{O}_{12} model on a $64 \times 64 \times 64$ simple cubic lattice with $x = 0.25$, log-log plot. The data set shown with + symbols was obtained from a series of 4 states which were obtained after cooling slowly from high temperature. The other data sets were obtained with a cold start initial condition. The solid line has a slope of -3.00 , and the dashed line has a slope of -2.00 .

FIG. 6. Angle-averaged magnetic structure factor at large x and low T for the dilute random-anisotropy \mathbf{O}_{12} model on $L \times L \times L$ simple cubic lattices, log-log plot. The lines have a slope of -2.00 . (a) $x = 0.75$; (b) $x = 1.0$.

Fig. 1 Fisch PRB1

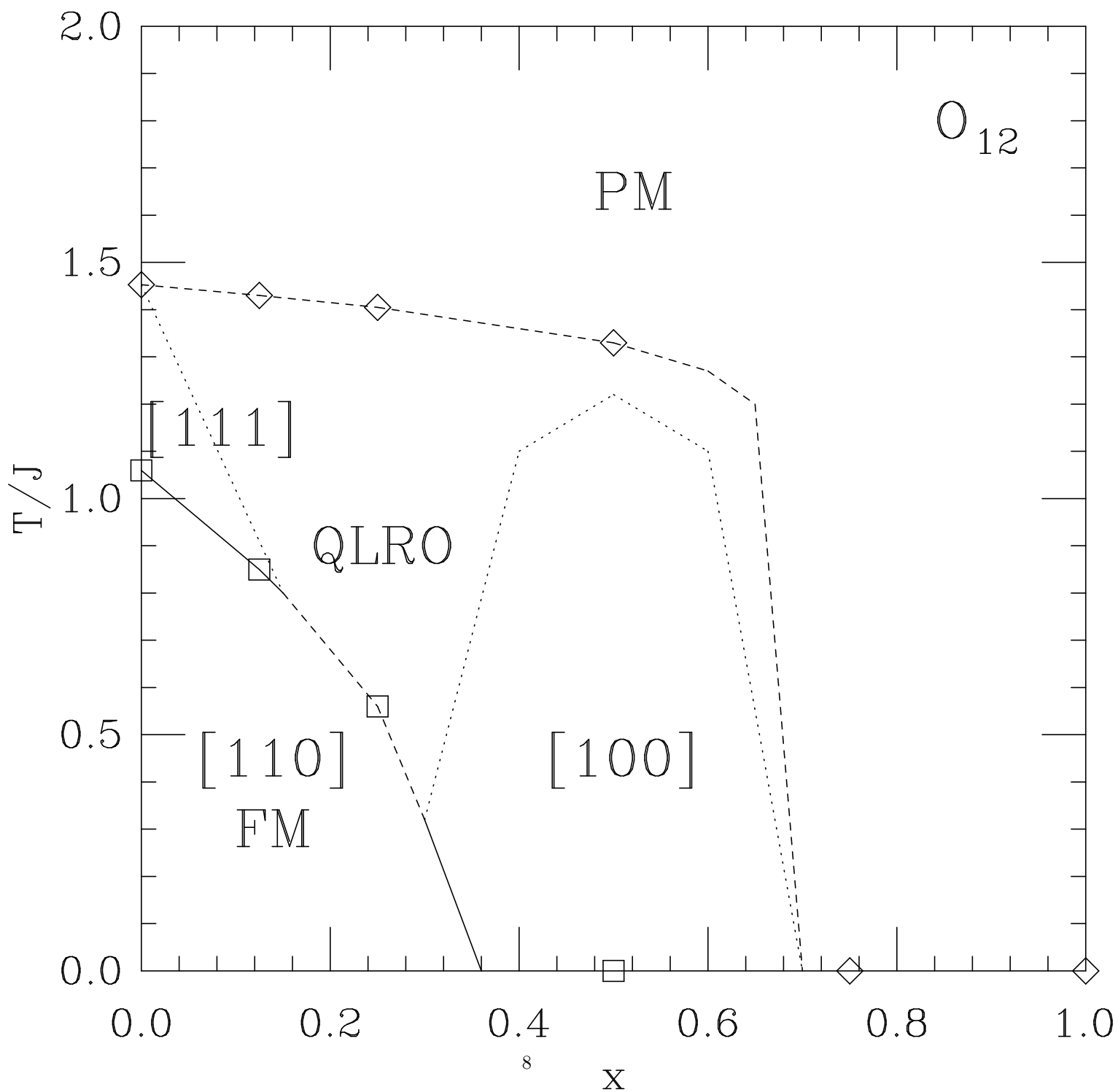


Fig. 2a Fisch PRB1

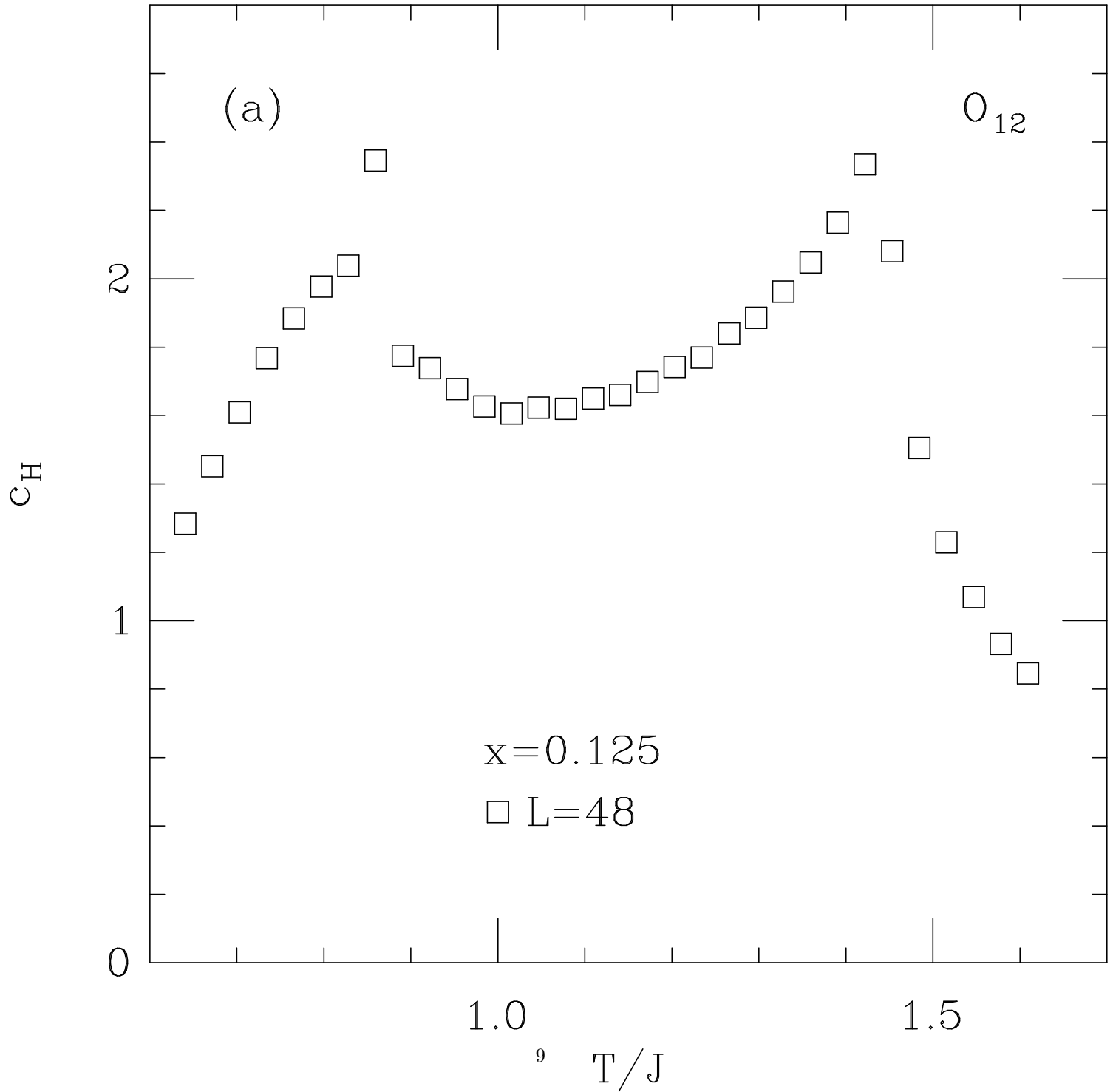


Fig. 2b Fisch PRB1

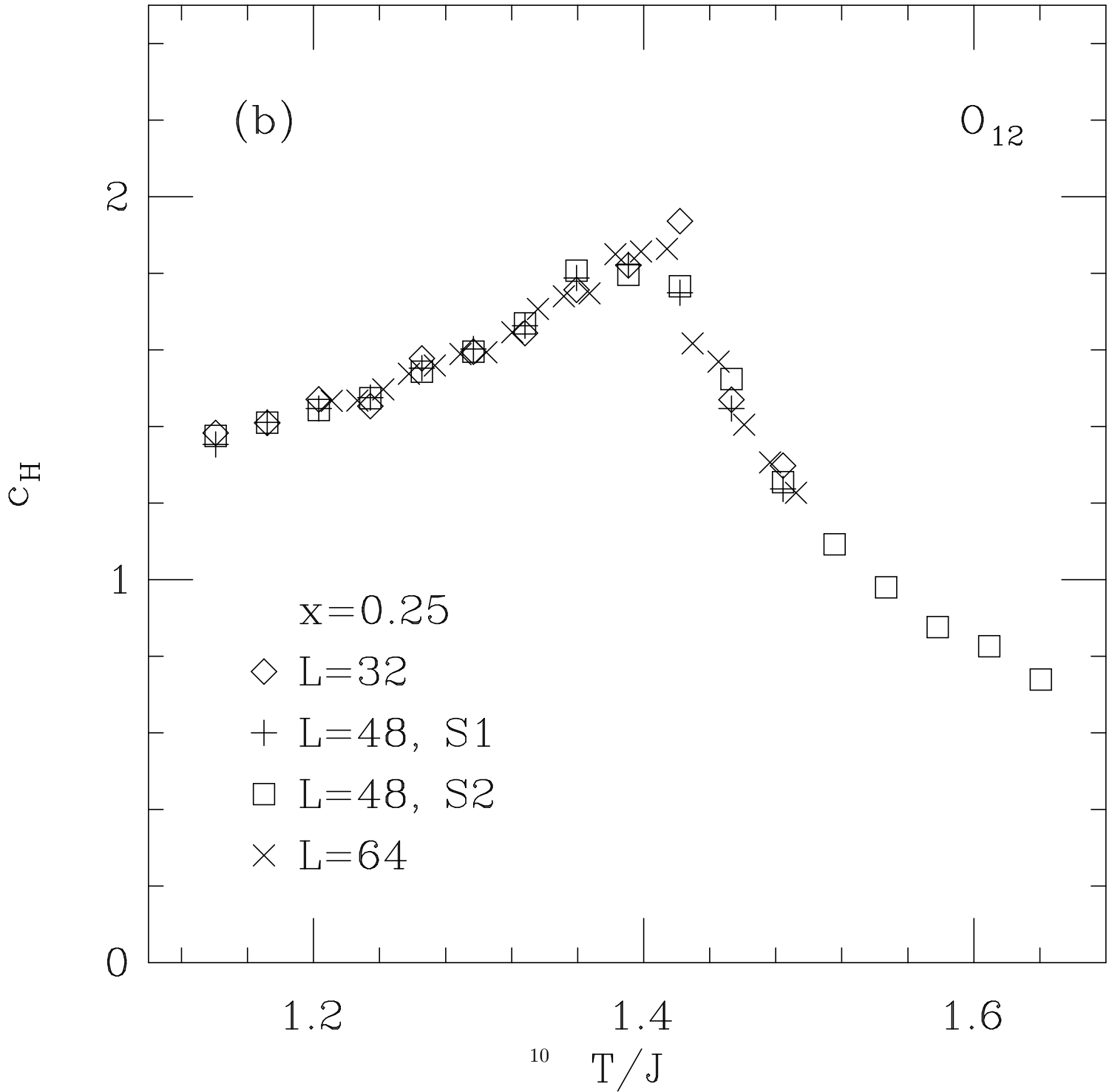


Fig. 2c Fisch PRB1

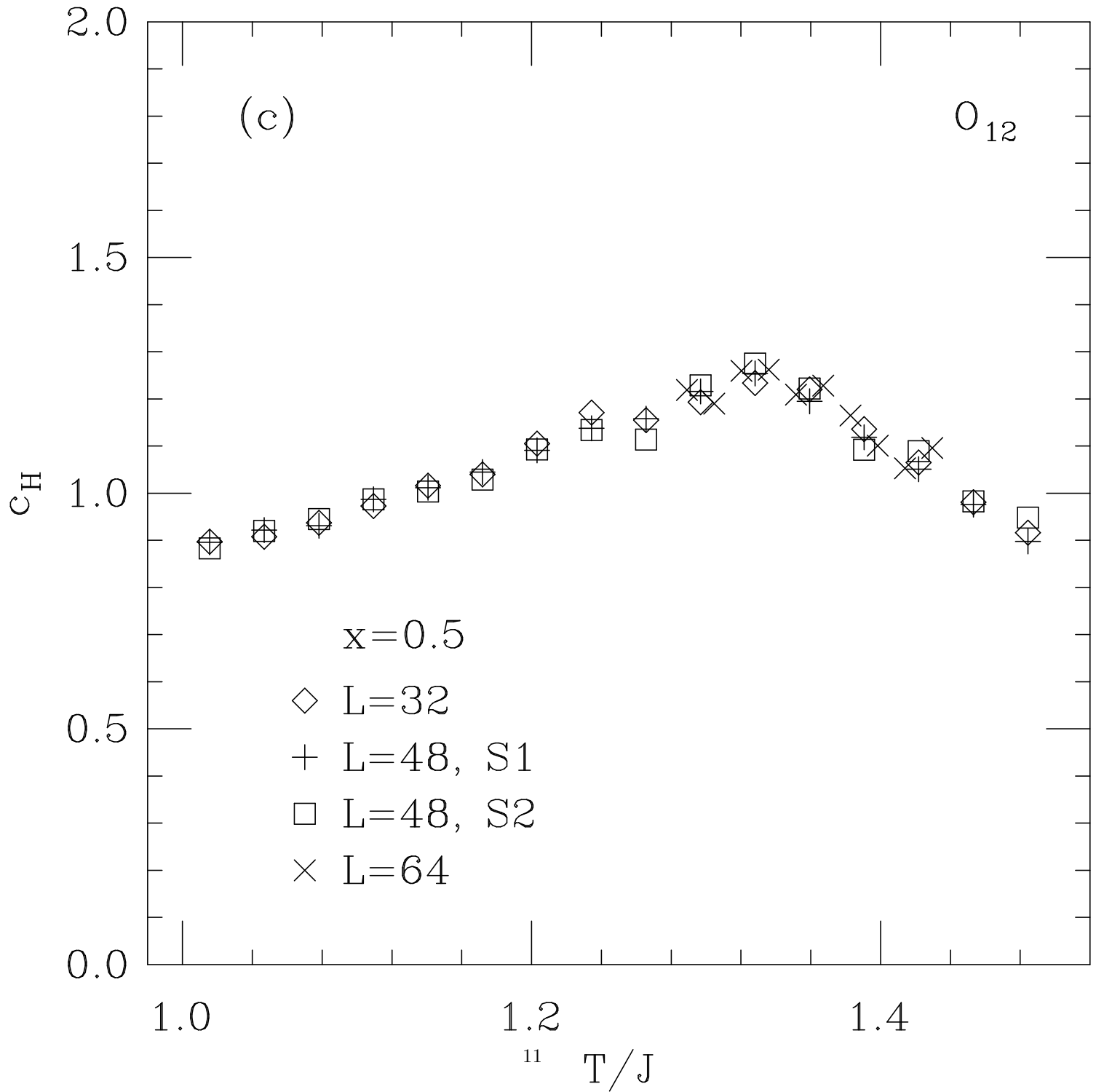


Fig. 3a Fisch PRB1

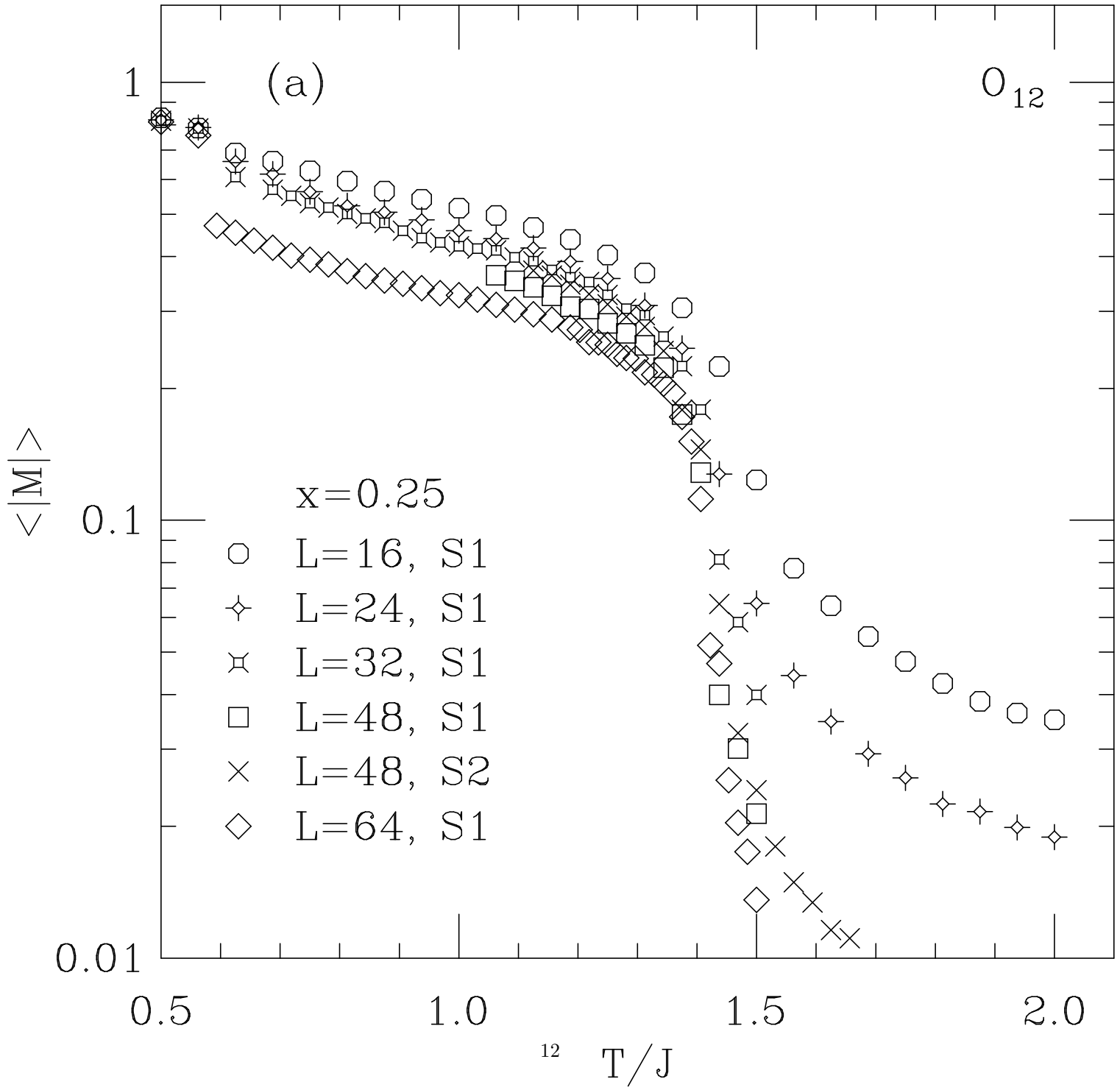


Fig. 3b Fisch PRB1

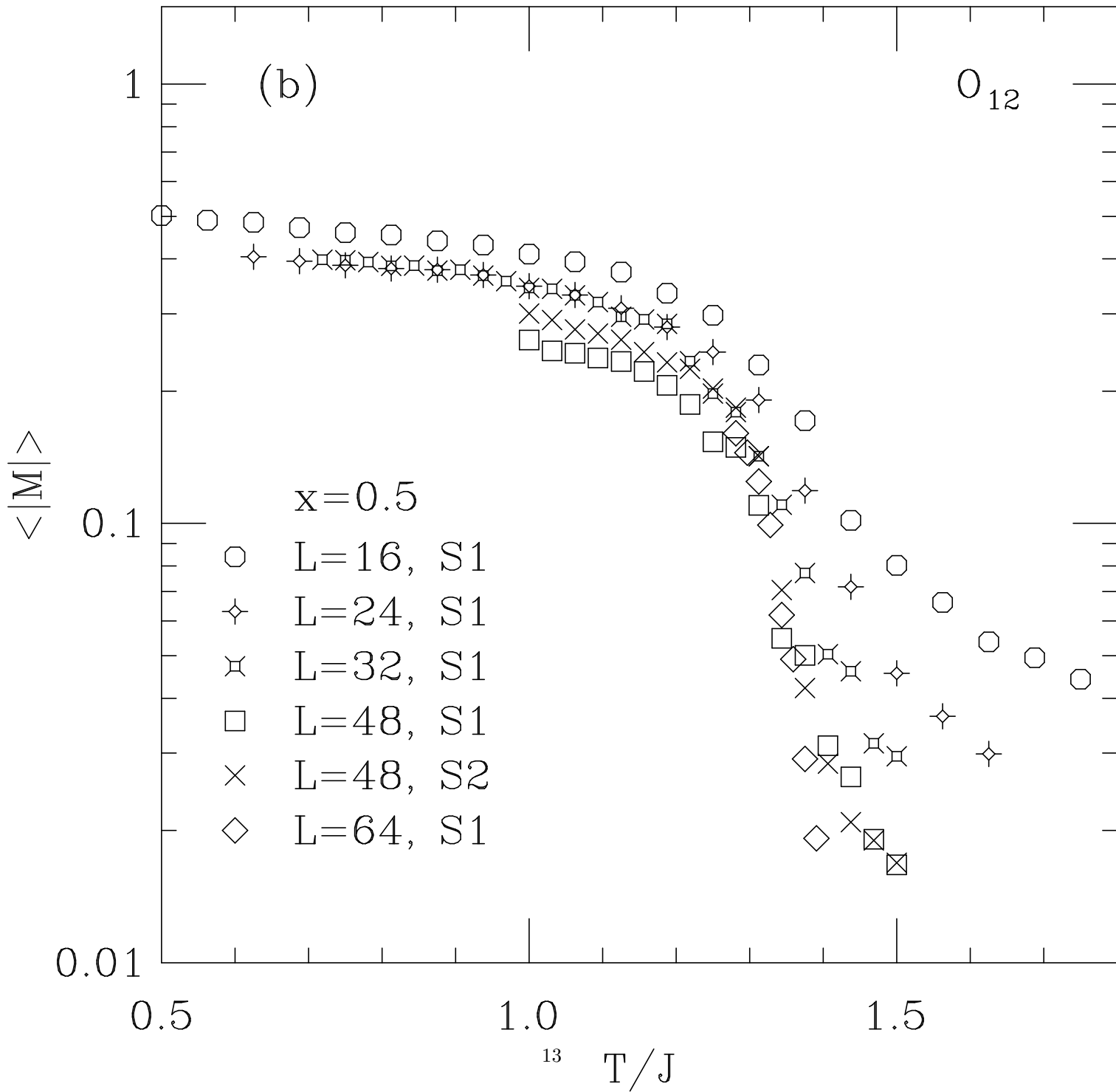


Fig. 4 Fisch PRB1

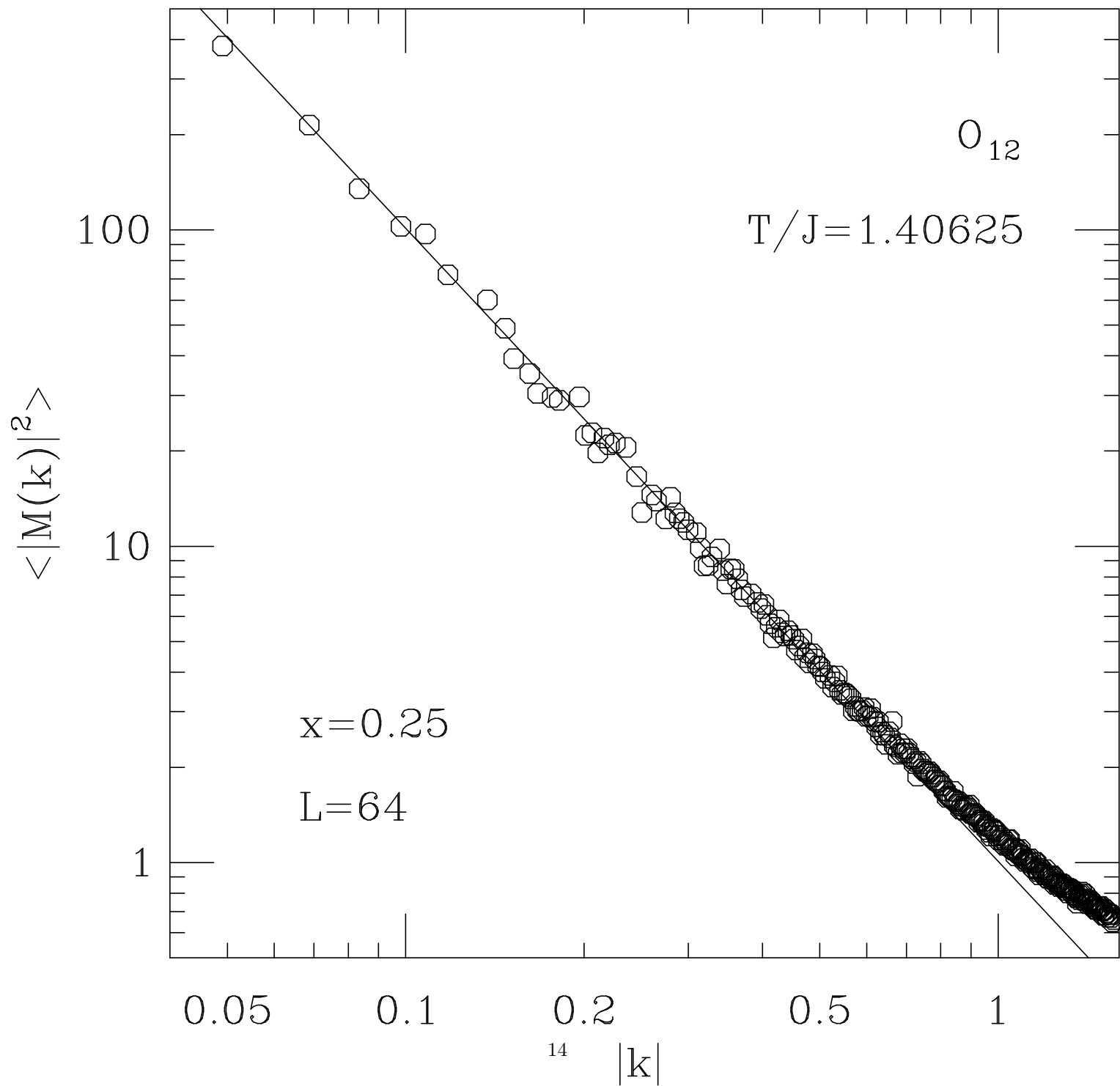


Fig. 5 Fisch PRB1

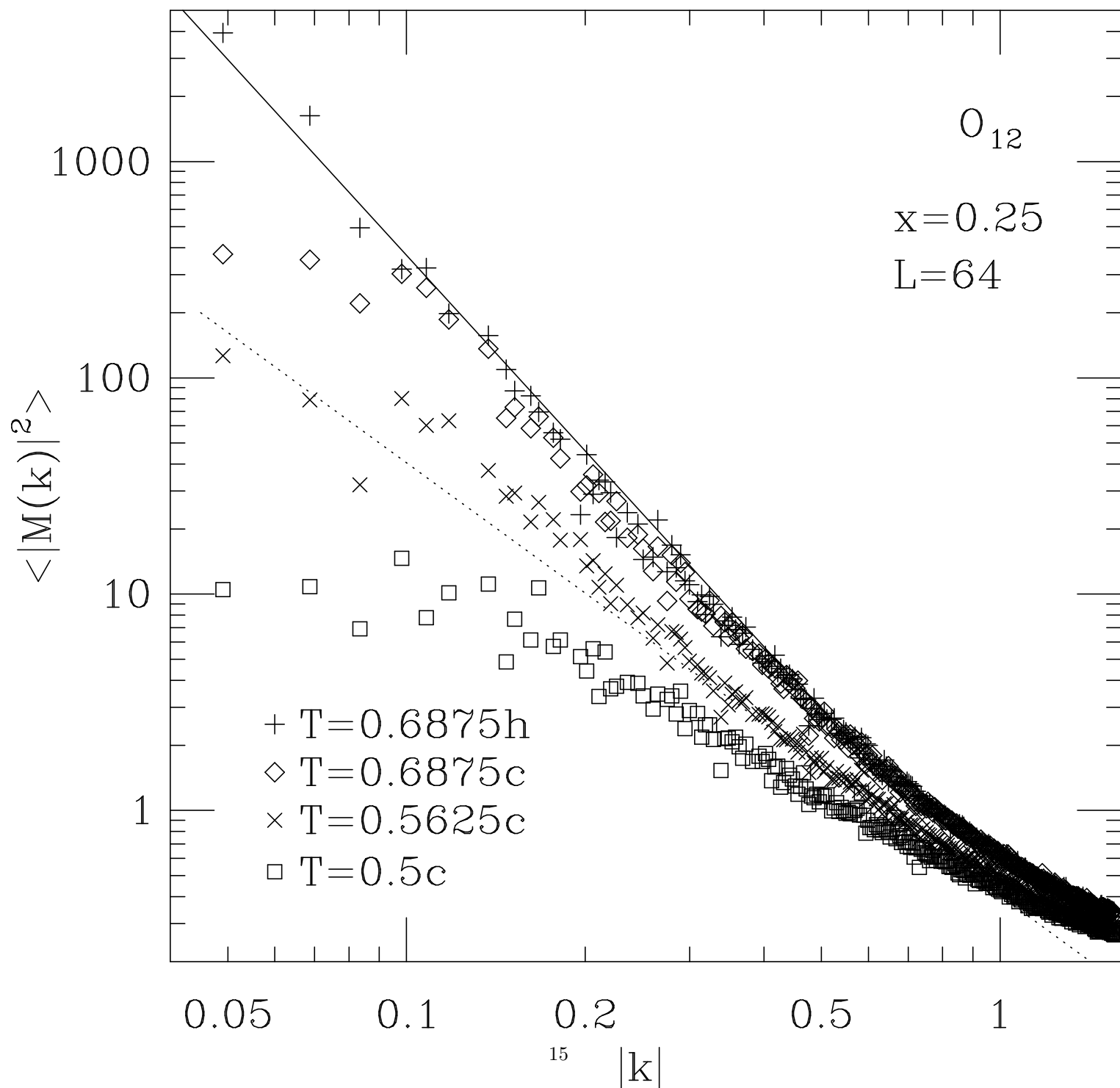


Fig. 6a Fisch PRB1

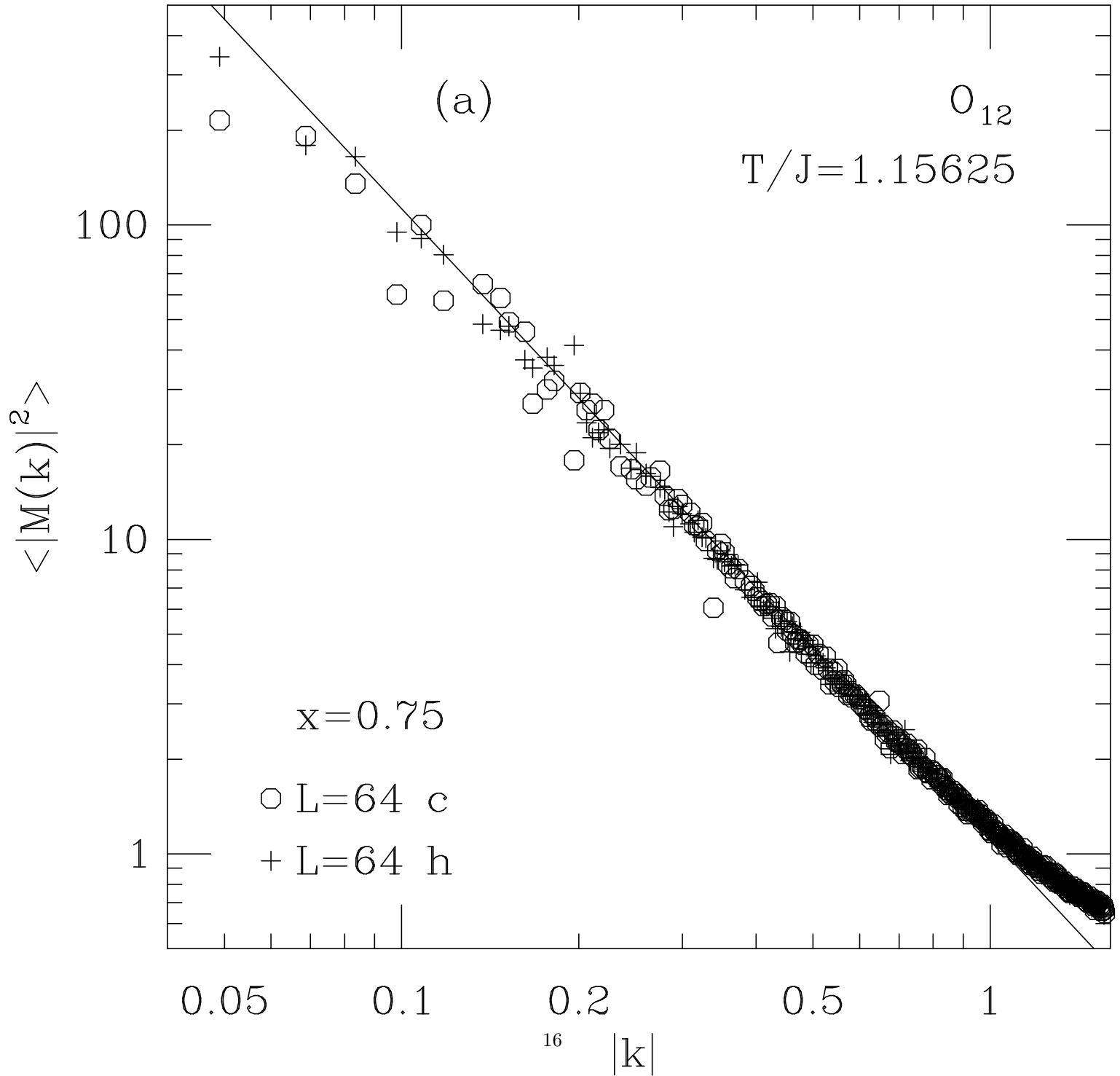


Fig. 6b Fisch PRB1

